International Conference on Space Optics—ICSO 2022

Dubrovnik, Croatia

3–7 October 2022

Edited by Kyriaki Minoglou, Nikos Karafolas, and Bruno Cugny,

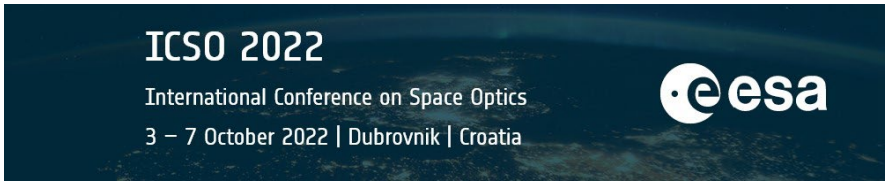

VERT-X: a new calibration facility for X-ray optics

International Conference on Space Optics — ICSO 2022, edited by Kyriaki Minoglou, Nikos Karafolas, Bruno Cugny, Proc. of SPIE Vol. 12777, 127770T · © 2023 ESA and CNES · 0277-786X · doi: 10.1117/12.2689013

VERT-X: a new calibration facility for X-ray optics.

A. Moretti[a], G. Pareschi[a], S. Basso[a], D. Spiga[a], M. Ghigo[a], G. Sironi[a], G. Tagliaferri[a], M. Civitani[a], V. Cotroneo[a], N. La Palombara[b], M. Uslenghi[b], M.Tordi[c], S. de Lorenzi[c], F. Dury[c], G. Valsecchi[d], F. Zocchi[d], F. Marioni[d], D. Vernani[d], F. Amisano[e], G. Parissenti[e], G. Parodi[f], M. Ottolini[f], P. Corradi[g], M. Bavdaz[g], and I. Ferreira[g]

[a]INAF-Brera, via Brera 28, 20123 Milan, Italy
[b]INAF-IASF-Milano, via Corti 12, 20133 Milan, Italy
[c]EIE Srl, Via Torino, 151 A 30172 Mestre (VE), Italy
[d]Media Lario, Via al Pascolo, 23842 Bosisio Parini (LC), Italy
[e]Apogeo Space, Borgo Pietro Wuhrer, 119, 25123 Brescia (BS), Italy
[f]BCV Progetti, via Sant'Orsola 1, 20123 Milan, Italy
[g]ESA-ESTEC, Keplerlaan 1, 2201 AZ Noordwjik, The Netherlands

ABSTRACT

The ESA Advanced Telescope for High-ENergy Astrophysics (ATHENA) will be the largest X-ray optics ever built. The ground calibration of its mirror assembly raises significant difficulties due to its unprecedented size, mass and focal length. The VERT-X project aims at developing an innovative calibration system which will be able to accomplish this extremely challenging task. The design is based on a 2.5 cm^2 parallel beam produced by an X-ray source positioned in the focus of a highly performing collimator; in order to cover the whole 2.5m diameter mirror, the beam is accurately moved by a raster-scan mechanism. The same device has the capability to tilt the beam by 3 degrees, in order to test both the off-axis performance and the out-of-field stray-light contamination. By design, VERT-X will be able to measure the ATHENA mirror half energy width (HEW) with a precision of 0.1", all over the field of view, with the source size, the collimator error and the raster scan tracking accuracy being the most important terms of the error budget. With respect to the traditional long-tubes, the VERT-X facility is much more compact. The entire system will be enclosed in a cylindrical 18m-high vacuum chamber with diameter ranging from 7m as maximum to 4m at minimum. Besides the smaller amount of involved resources, there are important benefits generated by the small scale design. First, it allows a vertical geometry which largely simplifies the mirror support and reduces to zero the PSF degradation due to the lateral gravity. Then, the location of the facility can be chosen flexibly and according to the project needs. Indeed, VERT-X will be built in continuity to the ATHENA mirror assembly integration facility, simplifying the verification and testing procedures. The VERT-X project, started in January 2018, is financed by ESA and conducted by a consortium that includes INAF, EIE, Media Lario, Apogeo Space (former GPAP), and BCV Progetti.

Keywords: Astronomy, X-ray, optics, ATHENA, calibration, facility

1. INTRODUCTION

The Advanced Telescope for High Energy Astrophysics (ATHENA) is the second Large mission of the ESA Cosmic Vision Science program, selected in 2014 to address *The Hot and Energetic Universe* science theme.[1] The ATHENA mission project successfully concluded the feasibility study (phase A) in November 2019 and, after a preliminary definition (phase B1), is now entering a reformulation phase. ATHENA will represent a powerful X-ray observatory for all astrophysics fields: the ambition of the mission will be the study of the Universe hot baryonic components, from the environment of the super massive black holes (SMBH) in the center of galaxies in the early Universe to the galaxy clusters and the large structures of the Cosmic Web. These goals will be achieved through the largest ever built X-ray mirror[2] which will focus 0.2-12.0 keV photons on two detectors, for

Send correspondence to A.M.
A.M.: E-mail: alberto.moretti@inaf.it

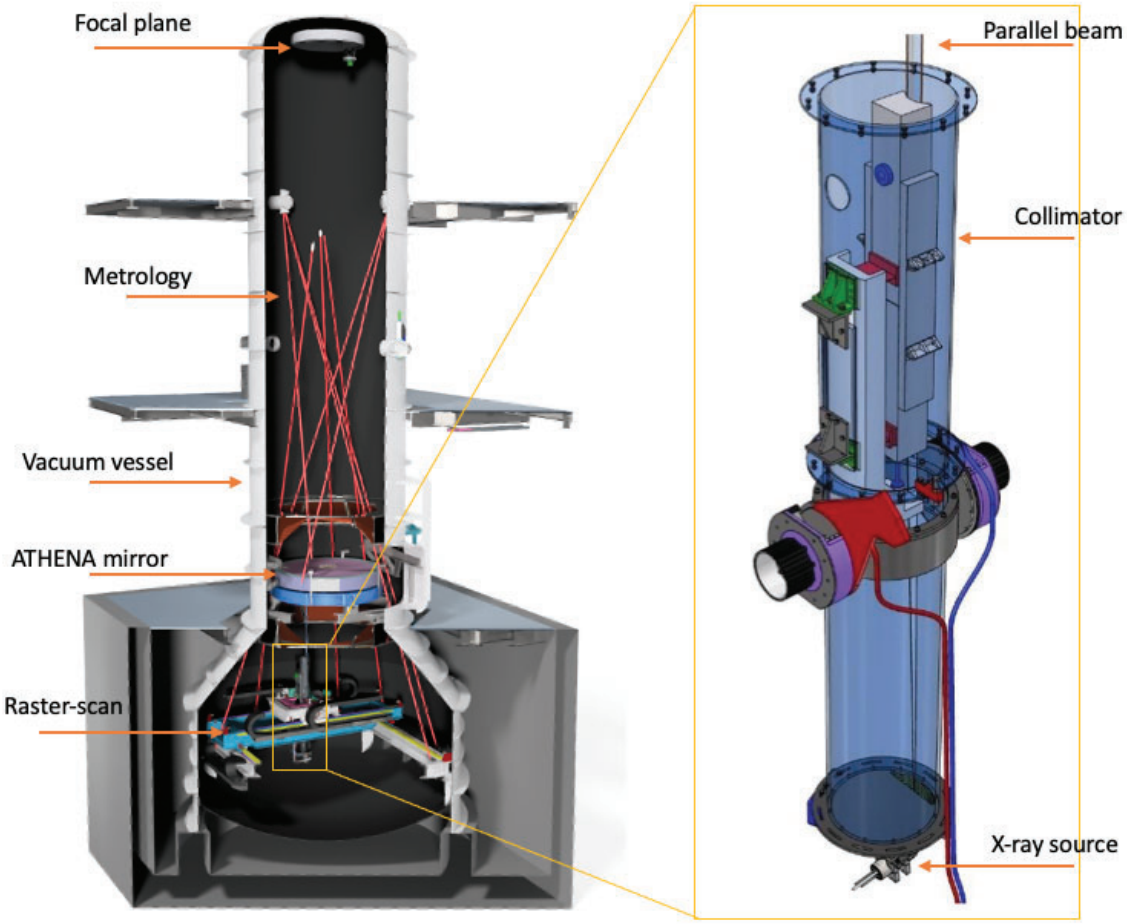

Figure 1. Design of the VERT-X facility, with the main parts in evidence. In the inset the zoom of the X-ray tube assembly (XTA) is shown. This tube hosts the parellelizing collimator and the x-ray source and represents the very core of the measure system.

spatially resolved high resolution spectroscopy (the X-ray Integral Field Unit, X-IFU) and for wide field imaging and low resolution spectroscopy (the Wide Field Imager, WFI) respectively. The mirror will be built using the ESA Silicon Pore Optics (SPO) technology which provides large effective area with excellent angular resolution.[3] While test and integration procedures of the single mirror modules (MM) have been well established[4–6] , the verification and calibration of the entire MA are particularly challenging and different options are still under scrutiny. In fact, to ensure that the uncertainties due to the divergence of the beam are compatible with the accuracy requirements of the calibrations, the source should be positioned at a minimum distance of 300 meters.[7] Since the largest X-ray calibration facility in Europe is the MPE Panter Lab, with a 120 m tube, this requirement could be satisfied only by a new X-ray long beam facility[8] or by a significant upgrade of the NASA X-ray & Cryogenic Facility (XRCF, https://optics.msfc.nasa.gov/).

In this paper we describe the design and the early development phase of the VERTical X-ray raster-scan facility for ATHENA calibration (VERT-X). VERT-X is an innovative concept, based on the idea of producing a parallel beam by means of a point-like source positioned in the focus of an highly performing X-ray collimator.[9] This concept has been already implemented in the BEATRIX facility[5] to test single mirror modules of the ATHENA optics. Since, for evident construction reasons, the beam amplitude has to be much smaller than the ATHENA mirror, the source-collimator system is thought to be moved by a raster-scan mechanism which covers all the

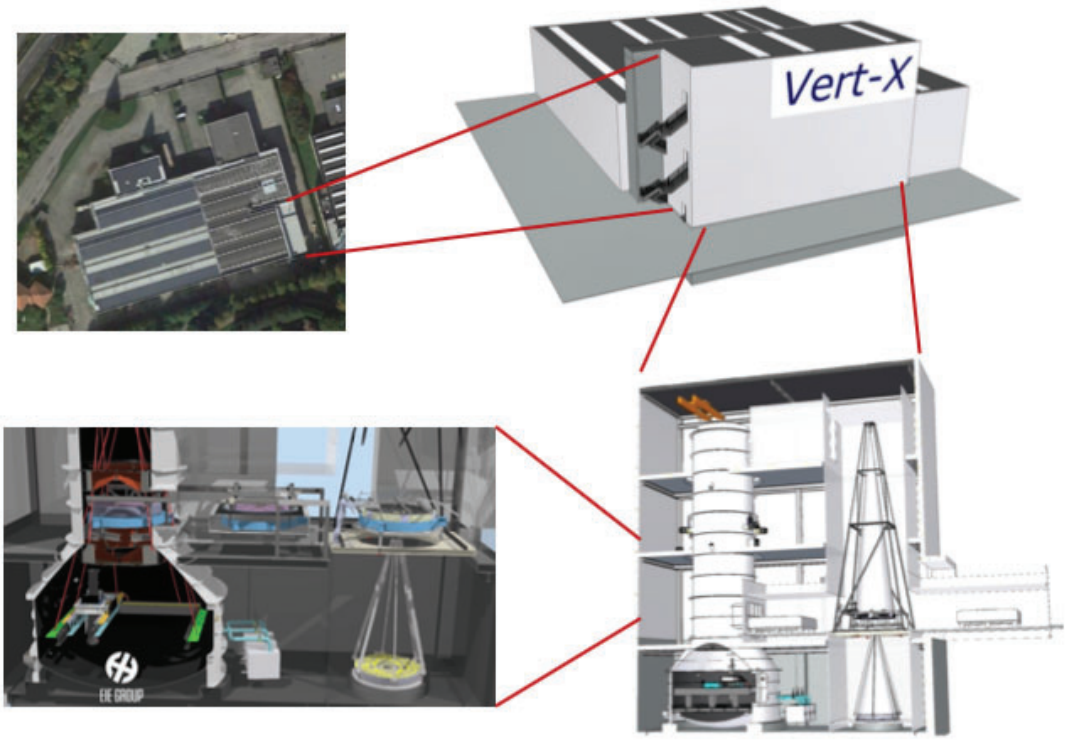

Figure 2. VERT-X location. The facility will be built in the same building of the ATHENA mirror integration facility, in the Media Lario premises. The ATHENA mirror assembly is moved between the two facilities by means of a trolley.

optics to be calibrated. This results in the design of a calibration facility much smaller in size (as shown in Fig. 1) with respect to the traditional long tube. The system is enclosed in a 18m-high cylindrical vacuum chamber, with the focal-plan on the top. The ATHENA MA will be positioned at the ground level. The raster-scan mechanism is positioned below that, at ~ 5 m underground , completely enclosed in the vacuum chamber, with the purposes of translating and rotating the vertical tube on which the X-ray source and the beam collimator are mounted (Fig. 1).

VERT-X has many different aspects from a traditional long-tube calibration facility design. First, it can produce a beam with such a low divergence which is far beyond the capabilities of long tube laboratories. Moreover, the VERT-X design compactness comes with important benefits besides the smaller amount of involved resources. The vertical geometry largely simplifies the mirror support and reduces to zero the PSF degradation due to the lateral (perpendicular to optical axis) gravity; the small size of the beam allows to characterise the contribution of the single modules to the over-all mirror performance; finally the location of the facility can be chosen flexibly, according to the project needs (Fig. 2). Indeed, VERT-X will be built in the same building of the Media Lario company, where the ATHENA MA integration facility[6] is already located. This, of course, would make the direct verification of the performance of the assembled optics much easier during the integration phase.

The VERT-X project was kicked off on January 2019 with an ESA-INAF 18-month contract with the goal of producing a detailed design of the entire facility. The first output of this activity has been presented in[10] . This activity was successfully concluded in July 2020. In November 2020 a new contract was issued, with the goal of developing those that in the previous phase have been evaluated as the most critical parts of the whole system. The final aim of this 24-month activity, is to test the real performance of this innovative measuring system[11] .

2. VERT-X MAIN COMPONENTS

In the following sections we present the most important and critical subsystems of the facility: the raster-scan, the X-ray source and the parallelizing collimator (Fig. 1).

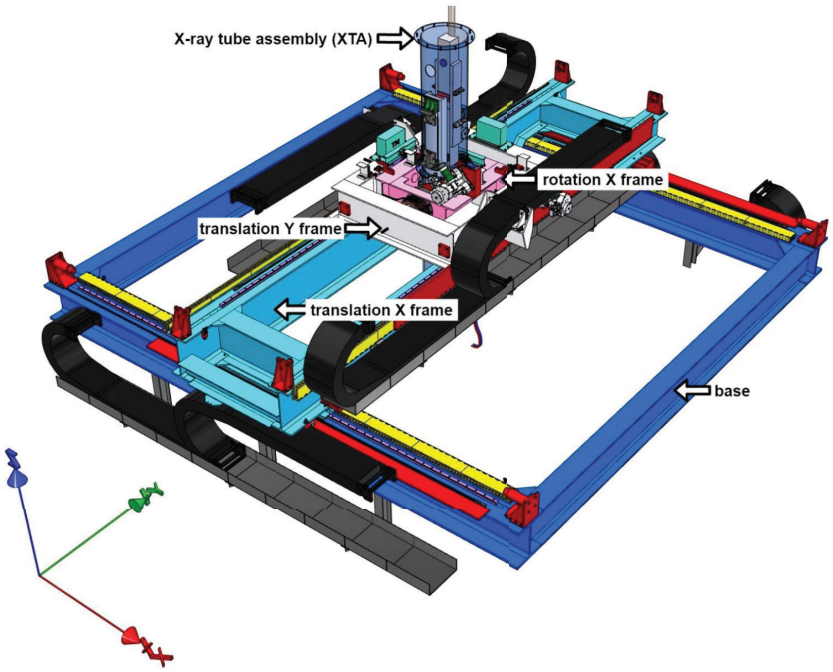

Figure 3. 3D view of the raster-scan mechanism with the main parts highlighted.

2.1 Raster-scan

The raster-scan mechanism allows the collimated X-ray beam to perform four movements, two translations on the horizontal plane and two tilts around the two horizontal axes. It consists of the following main parts: the base, the X and Y-axis translation frames and the tube also called the X-ray tube assembly (XTA) (Fig. 3) . All these elements are designed in the same material (AISI 304 stainless steel) in order to have the same thermal behaviour as the vessel and to ease the mechanical interfaces.

2.1.1 The translation and rotation frames

The base is the fixed part of the system: it is linked to the thermal vacuum chamber (TVC) and supports the X-axis translation frame, which consists of a bridge joining the base sides parallel to the X-axis. The translation along the X-axis is achieved by moving the bridge on top of the base. Y-axis translation frame consists of a trolley with actively cooled iron-less linear motors. The trolley constitutes the fixed part of a gimbal mount which allows the vertical tube (which carries the X-ray beam) to rotate around X and Y axes. The X side of the gimbal mount hosts the elements responsible for the rotation around the Y-axis of the vertical tube XTA. On the four supports that define the XTA rotation X and Y a coaxial double rotation system is installed. The XTA pointing within the field of view ($\lesssim$ 20 arcmin off-axis) is enabled by a flexure system. The coaxial double rotation system has the following advantages. It allows the tube pointing without over-stressing the flexures, so guaranteeing an unlimited number of pointings in the range 20-180 arcmin; with the upper limit due to the mechanical interference of the tube with the TVC. At the same time the pointing and tracking performances are still guaranteed in the field of view. The vertical tube assembly is the very core of the raster-scan, hosting the two main elements: the X-ray source and the collimator. These two elements are pieced together in a stainless-steel round tube to get the best rigidity between them (see the inset of Fig. 1). The tube itself is inserted in the axis assembly and positioned in order to be well balanced with the help of counterweights: balancing counterweights assure the COG centring along the X-Y axes, while the centering along the Z-axis is achieved moving the tube up and down.

2.1.2 Tip-tilt metrology and tiltmeters

A tip-tilt metrology system has been introduced in the design to provide the measurement of the XTA attitude variation. This is used by the control system to correct the pointing set-point in real-time, keeping the alignment of the X-ray beam within the required error range, so to minimize the beam divergence and consequently the raster scan contribution to the HEW measure error budget . The systems developed for the ALMA sub-mm

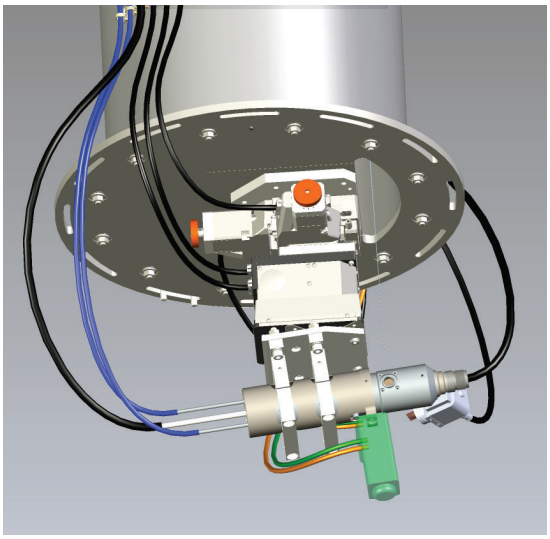

Figure 4. The X-ray source assembled on the XYZ stage, at the bottom of the vertical tube (XTA).

telescope[12] is the baseline. These are servo-actuated tilt-meters, based on an inverted pendulum kept in position by means of electro-magnetic motors and a position feedback provided by capacitive sensors. Furthermore, the inverted pendulum is combined with an inertial rotor, which can rotate almost freely around its rotational axis, constrained by a very weak flexure. The inertial rotor has zero DC gain, and it is sensitive to inclinations only above its self-resonance frequency: the real advantage of using both mechanism combined, consists in the possibility to filter out the disturbances of the inverted pendulum by means of the rotor readings. This is particularly relevant for VERT-X, where we expect to continuously have micro-accelerations due to the rail roughness, servo-control imperfections, stick-slip occurring at the pads level. The tilt-meters have been operating on-board the 25 European antennas of the array since 2013, for a total of 50 tilt-meters. No failures have been reported so far.

2.1.3 Raster-scan operations

The nominal scan velocity is 30 mm/s. Since the beam size, orthogonal to the scan direction, is 60 mm (see below), to cover the ATHENA MA a the total path of $\sim$ 100 m is needed. This corresponds to $\sim$1 hr accounting for $\sim$15 s of settling time at the start and end of each row (Fig. 5). The tube can be tilted not only to cover all the field of view (radius 20'), but also to point up to 3° off-axis in order to simulate the stray-light contamination from an off-axis source. In particular, this number is sized in accordance with what expected without baffles.[13] The main factors contributing to raster-scan tracking error are the thermal deformation due to temperature gradient along the raster scan structure and the non-repeatable runout of the trolley liner guide support system. In both these cases the metrology is expected to provide a correction leaving a residual uncertainty of 0.03".

A third error source is the gimbal and tube axis torsions due to the bearing friction on one side and the motor to the other side; in order to compensate for this error the gimbal and tube motors were doubled in order to apply a symmetrical axis torque. The error calculation has been performed through detailed simulation of calibration measures. Simulations are based on a proprietary tool by EIE called ErrorCalc, used for the design of astronomical telescopes, which has been updated and adapted for the purposes of VERT-X. Output of the simulations are reported in terms of the cumulative probability of the RMS pointing error in the various test

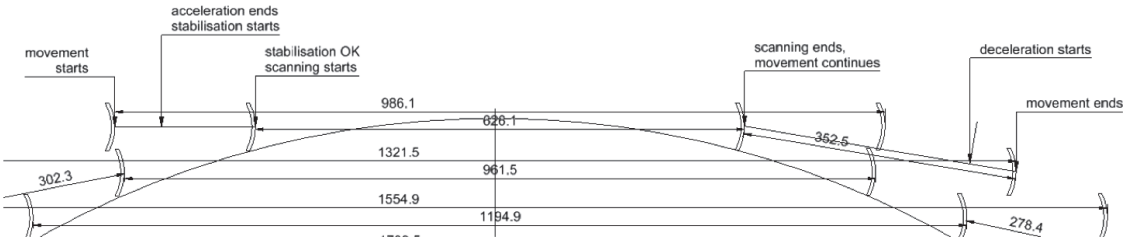

Figure 5. Scheme of the raster scanning pattern.

sessions. The median of the curve (0.56") is the final error estimation to be compared with the specification limit of 1". The figure shows that the error RMS is below the specification limit, thus the proposed raster-scan design is acceptable, with a scan velocity in the of 10-30 mm/s range.

2.2 The X-ray source

In the VERT-X design the X-ray source requires particular attention. First, different from the standard, the VERT-X source is required to have very small size (micro-focus): to keep the beam divergence in the order of 1", at a distance from the collimator of $\sim$ 2m, the size of the source should be $\lesssim$of 10μm. Then, the system has to fully operate in vacuum, which means the need of a liquid-based cooling system. Moreover, the system must

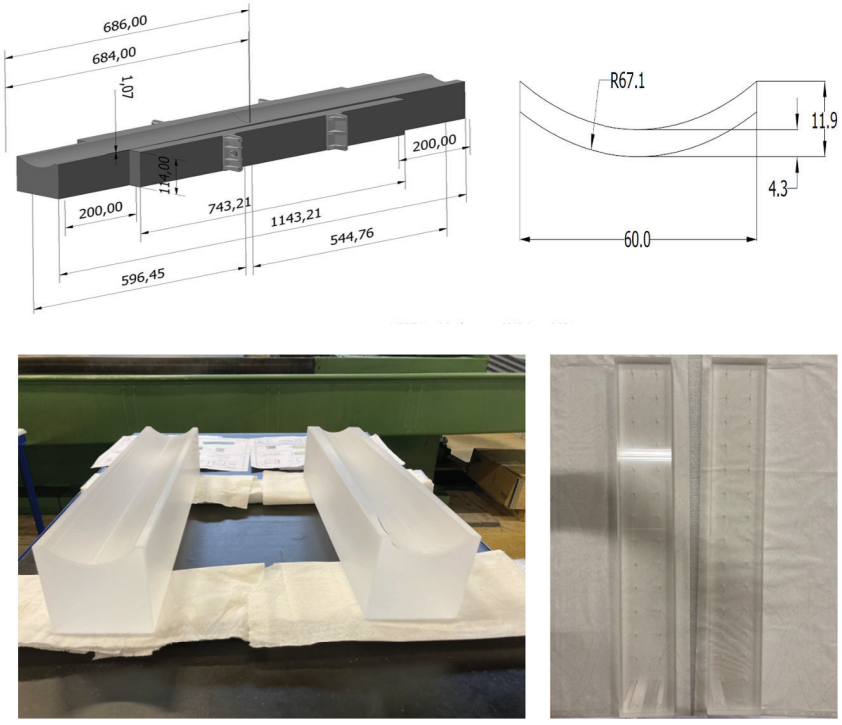

Figure 6. Mechanical design of the collimator, together with the beam footprint.

not cause vibrations on the raster-scan mechanism and this can only be achieved by an ion-pump for the high vacuum inside the source tube. These non-standard characteristics are provided by the SIGRAY FAAST source, a micro-focus sealed tube with a diverging beam refocussed by a double parabolic mirror in order to minimize the apparent source size. With respect to the standard product, the source is provided with a customized Be

window, 8μm thick, in order to extend the energy band down to values lower than 1 KeV. The source brightness profile at the exit of the double-parabolic mirror is expected to be Gaussian with a FWHM of 8 μm, as best effort. This corresponds to a divergence of the beam the order of 0.7", when positioned in the mirror focus at 2 m distance (see next Section). Two targets of different material, Tungsten and Chrome will be available at the anode. In the integration scheme the collimator will be fastened to the tube, while the X-ray source will be movable in order to be always positioned in the collimator focus. Movement along the 3 axis will be provided by a combination of three linear stages, according the configuration shown in Fig. 4; the linear motors have a travel range of 26 mm in the 3 dimensions with a minimum incremental $<1\mu$m.

2.3 The collimator

The optical design of the X-ray collimator is based on a Wolter I configuration of about 1.1 m in length and an average grazing incidence angle of about 0.4°. The main driving requirements that led to the definition of the design are related to the needs of sufficiently high reflectivity in the spectral range 0.2-12 keV and the limitation to $\lesssim$1" for the divergence error of the collimated beam produced by the mirror. The reflectivity requirement limits the average grazing incidence angle to less than 0.4°. Moreover, since micro-focus X-ray sources have dimension limited to $\sim$10 μm FWHM, the divergence requirement, in turn, limits the minimum distance between the source and the optics to about $\gtrsim$ 2m. Given the above constraints, a design, based on a Wolter I configuration, has been derived,[10,11] . An alternative possible design may consist of a section of a parabolic mirror, similar to the case of BEATRIX.[5] As discussed in[10] the Wolter design has been preferred due to the lower collimation sensitivity to alignment and source dimension. Mirror mechanical design consists of two separate sections for the parabolic and hyperbolic profiles of the Wolter collimator, respectively (Fig. 6). This solution is preferred to the monolithic

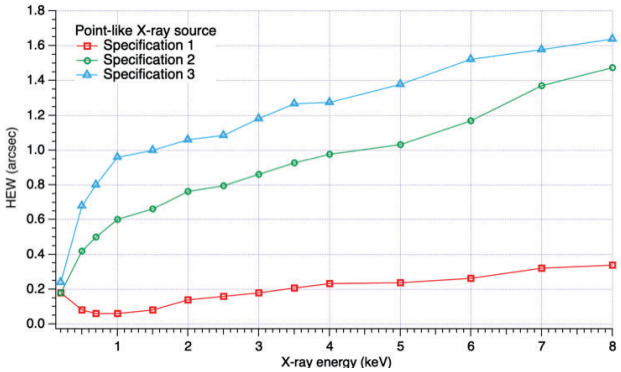

Figure 7. The HEW expected at different energies. Three different models are shown, with the blue one being our goal.

collimator approach for several reasons. First of all, the production of two independent shorter and lighter mirrors reduces the manufacturing and handling risks. Then, the relative alignment tolerance between the two collimator sections is loose enough to be accurately achieved by means of CMM metrology. Finally, the alignment of the parabolic and hyperbolic sections might be actively controlled either off-line (periodically or during calibration) or on-line (in real time in closed loop control). After alignment, the two mirror parts are held together by means of two plates of the same material of the optics, laterally fixed with adhesive. Alignment tolerances of the parabola to the hyperbola have also been studied investigating the impact of the displacements in the 6 degrees of freedom, 3 translational and 3 rotational.[14] To quantify the tolerable roughness and figure errors at different spatial scales, we started from the final polishing status of the BEaTriX mirror PSD as reference.[4] We assumed a similar polishing level at high frequencies, but a much smoother behaviour at mid- and low frequencies. This would correspond to a better figure error. This is reasonable, owing to the better quality asked for the VERT-X mirror, with respect to that of BEaTriX (a 3-fold improvement in the HEW). We have so generated a variable number of random profiles compatible with the considered PSDs. The expected HEW values are reported in Fig. 7 for increasing X-ray energy up to 8 keV.

In order to choose the material, an analysis to understand the roughness behaviour under the Ion Beam Figuring (IBF) action has been performed (Fig. 8). Two different glassy materials have been scrutinized: Zerodur®

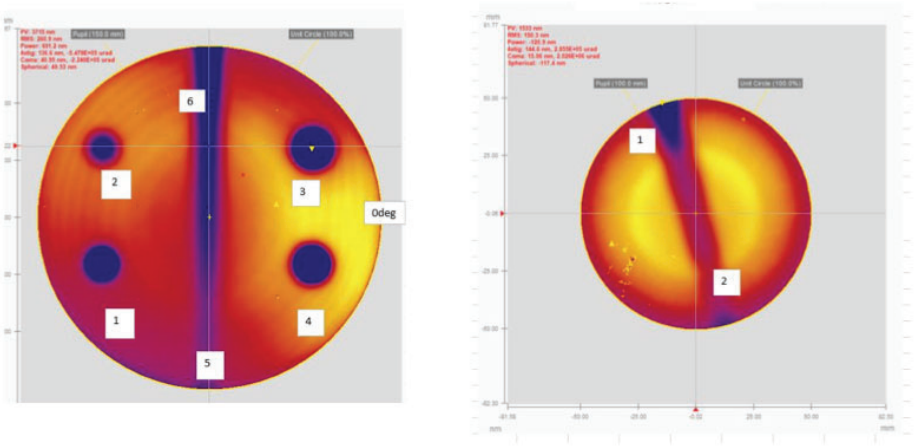

Figure 8. Two fused silica samples used in the analysis performed to study the IBF impact on material roughness.

and Cornig® 7980. The Cornig® 7980 fused silica was the final choice, with both materials being largely compliant with our requirements.

2.4 Raster scan tube / mirror interfaces

The design of the interfaces between the raster-scan vertical tube and the mirror entailed particular attention. The point is that, in case of rigid connection between mirror and tube, even a small elongation of $\sim 10\mu$m produced by a 1 deg temperature increase, would yield collimator deflections of 36.3 μm (peak-to-valley). This would produce a dramatic increase of the beam divergence at the level of 24.5" (HEW) . Therefore avoiding that the collimator becomes a sort of tube strengthening is mandatory. The collimator should act just as a load for the tube. Collimator deformations triggered by tube deflections should result as much as possible in rigid body movements, without appreciable distortions. To achieve this result the collimator interfaces have to realize a quasi-kinematic mount, which can be obtained by proper flexures. At the bottom, the collimator axial support is aligned with collimator CG (Fig. 9). This system is expected to decouple tube and collimator structural behaviour. All interfaces connected to the collimator are designed in Invar to reduce CTE mismatch of the components rigidly connected to the collimator. In order to reduce the impact of flexures quasi-kinematic collimator mount on the tube design and to simplify the collimator integration procedure, an intermediate structure level, between collimator and tube has been foreseen. This is an L-shaped structure which allows to manipulate the interfaces in a more comfortable way (Fig. 9). Moreover the presence of an intermediate interface significantly reduces the time needed for the mirror-tube integration, with important programatic benefits. The cost of this additional interface is the mass increase. Collimator integration in vertical position appears to be the most suitable solution. An integration with horizontal collimator would need at least one force actuator to mitigate the lateral gravity distortions. Vertical integration also avoids any flexure spring back during operation, since integration and operative configurations are almost the same. Very fine alignment between tube and collimator axis is not needed since small residual misalignment can be compensated by the tube verticality setting.

3. THE HEW ERROR BUDGET AND THE CRITICAL PARTS

According to the ATHENA Calibration plan, an absolute knowledge error (AKE) of 0.1" at 68% confidence is required for the MA HEW at all energies in the 0.3-12.0 KeV energy band all over the field of view.[7] This has been the main driving factor in the VERT-X design.

The PSF observed at VERT-X, $\mathrm{PSF_{VTX}}$, will be given by the convolution of the ATHENA MA intrinsic PSF $\mathrm{PSF_{MA}}$, with the residual beam divergence $\mathrm{PSF_{BEAM}}$. Therefore the observed $\mathrm{HEW_{VTX}}$ will be given by

$$\mathrm{HEW^2_{VTX}} = \mathrm{HEW^2_{MA}} + \mathrm{HEW^2_{BEAM}}. \quad (1)$$

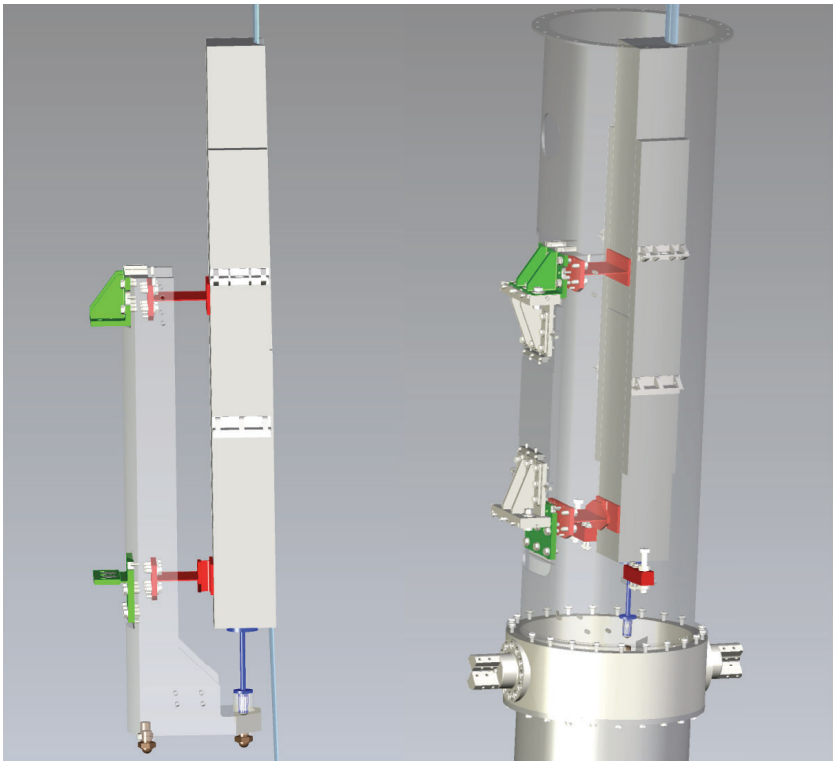

Figure 9. The collimator assembly, alone on the left and mounted on the raster-scan tube on the right.

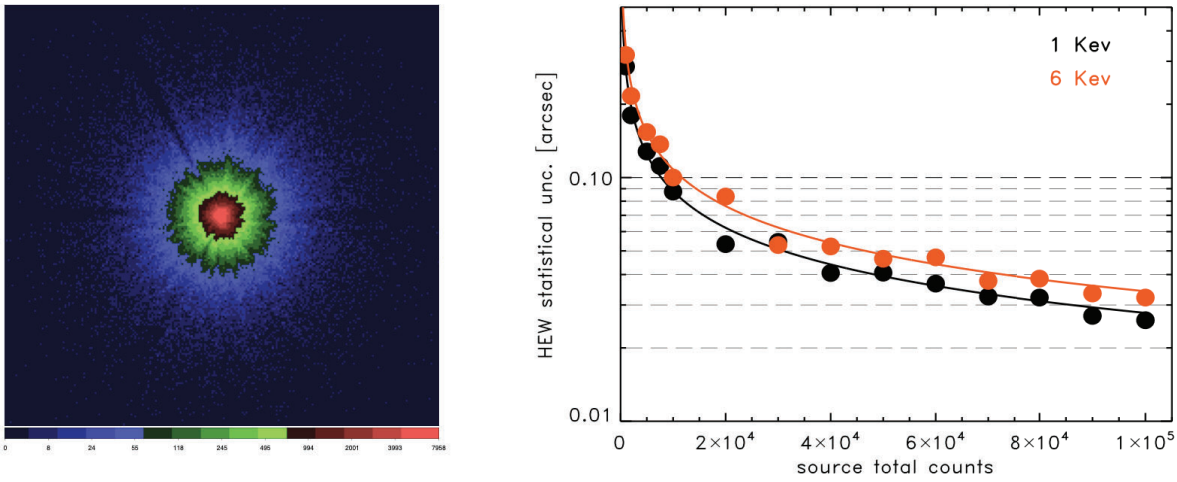

Figure 10. The simulated ATHENA PSF (left panel), assumed to calculate the statistical uncertainty on the HEW measure, as function of the accumulated events (right panel).

Simply from the error propagation, it follows that the uncertainty on the $\mathrm{HEW_{MA}}$, which is the goal of verification/calibration, will be given by

$$\sigma^2_{\mathrm{MA}} = \frac{\mathrm{HEW}^2_{\mathrm{VTX}}}{\mathrm{HEW}^2_{\mathrm{MA}}}\sigma^2_{\mathrm{VTX}} + \frac{\mathrm{HEW}^2_{\mathrm{BEAM}}}{\mathrm{HEW}^2_{\mathrm{MA}}}\sigma^2_{\mathrm{BEAM}} \quad (< 0.1”). \tag{2}$$

The first term of the quadratic sum ($\sigma^2_{\rm VTX}$) is the statistical error, the second the systematic ($\sigma^2_{\rm BEAM}$). Using Eq.4 we can re-write 3

$$\sigma^2_{\rm MA} = (1 + \frac{\rm HEW^2_{BEAM}}{\rm HEW^2_{MA}})\sigma^2_{\rm VTX} + \frac{\rm HEW^2_{BEAM}}{\rm HEW^2_{MA}}\sigma^2_{\rm BEAM}. \quad (3)$$

In this way, we put in evidence the key terms of the error budget: the statistical error $\sigma_{\rm VTX}$, the beam divergence $\rm HEW_{BEAM}$ and its uncertainty $\sigma_{\rm VTX}$. We note that the statistical error is weighted by a factor >1, while the systematic error by a factor <<1.

3.1 The statistical error

For a given PSF, the statistical error on the HEW measure directly depends on the (square root of) accumulated photons. In order to estimate the expected statistical error on the HEW of the ATHENA MA as measured at the VERT-X facility, we started from the ray-tracing output[15] shown in Fig. 10: this has been produced with 1.5×10^6events at 1 keV energy on axis and contains a full treatment of error terms: (i) in-plane and out-of-plane figure errors/response focal length/kink angle errors; (ii) reflection coating and surface roughness/scattering parameters; (iii) translational integration errors; (iv) rotational integration errors. As said, the PSF model allows us to estimate the expected statistical error in the HEW calibration as function of the number of photons collected during the calibration tests. To this aim, starting from the best fit model of the ray-tracing PSF we simulated PSF with different numbers of photons, ranging from 1000 to 100,000. At a given number of collected events we simulated 100 times PSF and measured the HEW. In Fig. 10, for each number of photons, we report the standard deviation of the 100 measures. As expected, the HEW measure accuracy follows the number of counts with a slope of 0.5. We find that, to keep the statistical uncertainty at the level of 0.05", corresponding to 50% of the total HEW error budget, ∼40,000 counts per energy bin are required. This statistical level is compatible with the VERT-X concept of operation with the main factor being the detector sustainable rate[10] .

3.2 The systematic error

The systematic term in the error budget, which is the beam divergence, is caused by several independent contributions. In the design phase (i) the source dimension $\rm HEW_{SOU}$, (ii) the mirror error $\rm HEW_{MIR}$, (iii) the raster-scan tracking uncertainty $\rm HEW_{TRK}$ and (iv) the relative heat-induced displacement between source and collimator $\rm HEW_{THR}$, have been individuated as the major ones:[10]

$$\rm HEW^2_{BEAM} = (HEW_{SOU} + HEW_{MIR})^2 + HEW^2_{TRK} + HEW^2_{THR}. \quad (4)$$

Therefore, the requirements on the ATHENA MA PSF calibration accuracy directly translate into requirements on these elements, which are considered the most critical part of the system. The expected values of the single terms of the systematic error budget have been estimated at the design level and are summarised here in Tab 1. Note that the source size combines linearly with the mirror error.[14]

Table 1. HEW systematic error budget estimated at the design level.

ELEMENT	VALUE	ERROR
$\rm HEW_{SOU}$	0.80"	0.16"
$\rm HEW_{MIR}$	1.0 "	0.20"
$\rm HEW_{TRK}$	0.27"	0.24"
$\rm HEW_{THR}$	0.10"	0.10"

Assuming an intrinsic HEW of 5.0" for the ATHENA MA and filling the equation with the numbers here reported, we find that in the nominal operations the expected measured HEW, will be 5.2", accounting for a 0.05" statistical error, as discussed in the previous Section. This would allow us to estimate the intrinsic $\rm HEW_{MA}$ with

an error of 0.096" at 68% confidence, just within the requirement. Among the different subsystems comprising the VERT-X facility those that mostly contribute to the HEW measure systematic error budget are considered the most critical.[11] These parts, namely the parallelizing mirror and the X-ray source, both mounted on the raster scan vertical tube, together with the raster scan rotation and translation frames are under development. The final assessment of their performance will be done by means of the laboratory measures of their contribution to the beam divergence. After the development and manufacturing, raster-scan tracking error (HEW_{TRK} in the previous Section) will be accurately estimated by a test campaign together with a first assessment of the displacement induced by thermal gradient on the vertical tube.

4. MEASURING THE BEAM DIVERGENCE

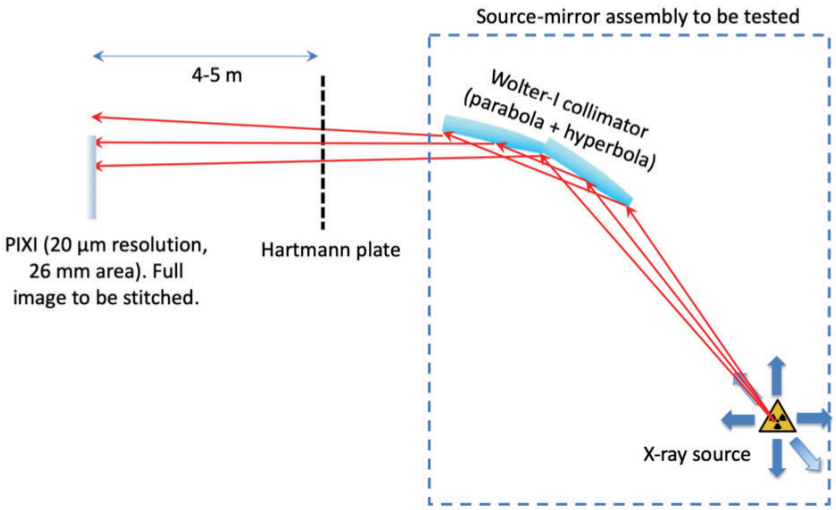

Figure 11. The experimental set-up to measure the beam divergence.

The contribution to the beam divergence produced by the source dimension (HEW_{SOU}) coupled with the collimator error (HEW_{MIR}), together with the final assessment of the term due to the thermal gradient along the tube (HEW_{THR}), will be tested at the PANTER facility. The scope of the test is to provide a demonstration of the collimating capabilities of VERT-X to the required level of about 1 arcsec. This requires the alignment of the X-ray source in the focus of the mirror. To this end, we aim for achieving the best alignment of the source to the mirror focus under X-rays, while the beam divergence is monitored with continuity until the minimum divergence is found. Due to the aberration mitigation in a double-reflection system, we expect that the residual divergence in the collimated beam caused by source misalignments will be very limited (no appreciable effect on beam aberration for lateral displacements < 0.5 mm). Although forgiving, this kind of alignment cannot be obtained in UV light, because the aperture diffraction would conceal the aberrations resulting from misalignments and fabrication errors. Alignment and test in X-rays, in contrast, represent a real at-wavelength validation of the concept, and allows us testing at the same time the optical properties of the Wolter-I collimator. Therefore, the alignment of the source to the mirror will have to be made in X-rays, when the facility is under vacuum. This can be achieved by means of the 3D linear motors previously described which shift the source spot. In the PANTER facility, the source is located 123 m away from the experimental chamber, but in this case, it will not be used because the Sigray source generates the beam to be tested itself. However, unlike the final VERT-X setup, the collimator will have to be set up in horizontal direction. Lateral gravity distortions during this test will be mitigated by an actuator force. Indeed, the tube has a hole for the actuator pusher passing. Actuator force will be adjustable around the nominal value obtained from numerical assessment, for a fine tuning on site during optical tests.

Once aligned, the parallel beam will be directed on the detectors available at PANTER. Since the source is not monochromatic, all possible energies (continuum + fluorescence lines of Chromium) will be collimated together.

In order to separate the contributions from different monochromatic components, TRoPIC is the most natural choice owing to its spectral resolution. Because TRoPIC has a field smaller (2 cm) than the expected size or the beam (6 cm), a stitching of different exposures will be necessary. The adoption of PIXI (20 μm) will be necessary whenever higher spatial resolution than that of TRoPIC (75 μm) will be mandatory. Indeed, sole observation of the collimated beam does not allow accurate measurement of the beam divergence. Therefore, a technique based on wavefront detection will be adopted.

Characterization of the collimated wavefront is a basic tool aiming at achieving the best alignment of the source to the collimating mirror and ascertaining the final achievable collimation degree assured by the source-mirror assembly. The concept we have in mind is displayed in Fig. 11 : a Hartmann plate (i.e., a metallic plate with a regularly-spaced grid of squared holes) is interposed between the mirror and the imaging detector. Selecting events in TRoPIC allows one to characterize the mirror at a given X-ray energy. The Hartmann plate samples the wavefront out of the collimating mirror, and the beamlets emerging from the holes are detected on the TRoPIC plane. If the collimated beam were a perfect planar wave, the pattern recorded by TRoPIC would be a perfect grid reproducing the sieve plate. Due to unavoidable imperfections, the centroids of the beamlets will be affected by displacements, from which the wavefront can be reconstructed and the kind and magnitude of the source displacement can be inferred and corrected. This presumes the pre-calibration of sieve plate itself by external metrology tools, in order to remove the imperfections in the hole placement. Once reached the minimum possible divergence, the measurement returns the expected HEW due to residual mirror defects (shape, and misalignment of the parabola wrt. the hyperbola). According the current schedule, the test campaign will be performed in the Q2 of 2023.

5. SUMMARY AND CONCLUSIONS

The ground verification and calibration of the ATHENA mirror assembly raises significant difficulties due to the unprecedented size, mass and focal length. We developed the design of a new facility capable of carrying out this task. The idea is based on the production of a parallel beam through a micro-focus source and a collimator that parallels the X-ray photons. The most compelling element in the project is the requirement on the PSF calibration accuracy. The design analysis identified the size of the source, the errors of the mirror, the raster-scan vertical tube tracking uncertainty and the relative displacement between source and mirror as the main factors in the systematic error budget of the PSF calibration. According to the preliminary assessment, at the design level, VERT-X measures will be compliant with the required accuracy with very tiny margin. In this paper we reported on the general design of the facility and on the current activity of the project consortium which is the first phase of the development of the core of the VERT-X measure system: the raster scan translation and rotation frames together with the XTA system which includes the raster-scan vertical tube, the X-ray source and the parallelizing collimator. The final goal of this activity, foreseen for Q3 of 2023, will be the laboratory test of the real performance of the most critical parts of this innovative calibration facility.

REFERENCES

[1] Nandra, K., "The Hot and Energetic Universe: A White Paper presenting the science theme motivating the Athena+ mission," *arXiv e-prints* , arXiv:1306.2307 (June 2013).

[2] Ferreira, I., Bavdaz, M., Ayre, M., Fransen, S., Pacros, A., Linder, M., Stefanescu, A., Branco, M., Guainazzi, M., Ness, J.-U., Oosterbroek, T., and Willingale, R., "ATHENA reference telescope design and recent mission level consolidation," in [*Society of Photo-Optical Instrumentation Engineers (SPIE) Conference Series*], *Society of Photo-Optical Instrumentation Engineers (SPIE) Conference Series* **11822**, 1182204 (Aug. 2021).

[3] Bavdaz, M., Wille, E., Ayre, M., Ferreira, I., Shortt, B., Fransen, S., Millinger, M., Collon, M. J., Vacanti, G., Barriere, N. M., Landgraf, B., Riekerink, M. O., Haneveld, J., Start, R., van Baren, C., Della Monica Ferreira, D., Massahi, S., Svendsen, S., Christensen, F., Krumrey, M., Handick, E., Burwitz, V., Bradshaw, M., Pareschi, G., Valsecchi, G., Vernani, D., Kailla, G., Mundon, W., Phillips, G., Schneider, J., Korhonen, T., Sanchez, A., Heinis, D., Colldelram, C., Torti, M., and Willingale, R., "ATHENA x-ray optics development and accommodation," in [*Society of Photo-Optical Instrumentation Engineers (SPIE)*

Conference Series], *Society of Photo-Optical Instrumentation Engineers (SPIE) Conference Series* **11822**, 1182205 (Aug. 2021).

[4] Basso, S., Salmaso, B., Spiga, D., Ghigo, M., Vecchi, G., Sironi, G., Cotroneo, V., Conconi, P., Redaelli, E., Bianco, A., Pareschi, G., Tagliaferri, G., Sisana, D., Pelliciari, C., Fiorini, M., Incorvaia, S., Uslenghi, M., Paoletti, L., Ferrari, C., Lolli, R., Zappettini, A., Sanchez del Rio, M., Parodi, G., Burwitz, V., Rukdee, S., Hartner, G., Müller, T., Schmidt, T., Langmeier, A., Ferreira, D. D. M., Massahi, S., Gellert, N. C., Christensen, F., Bavdaz, M., Ferreira, I., Collon, M., Vacanti, G., and Barrière, N. M., "First light of BEaTriX, the new testing facility for the modular X-ray optics of the ATHENA mission," *arXiv e-prints* , arXiv:2206.15468 (June 2022).

[5] Salmaso, B., Basso, S., Giro, E., Spiga, D., Sironi, G., Vecchi, G., Ghigo, M., Pareschi, G., Tagliaferri, G., Uslenghi, M., Fiorini, M., Paoletti, L., Ferrari, C., Beretta, S., Zappettini, A., Sanchez del Rio, M., Pelliciari, C., Burwitz, V., Ferreira, I., and Bavdaz, M., "BEaTriX: the Beam Expander Testing X-Ray facility for testing ATHENA's SPO modules: progress in the realization," in [*Optics for EUV, X-Ray, and Gamma-Ray Astronomy IX*], *Society of Photo-Optical Instrumentation Engineers (SPIE) Conference Series* **11119**, 111190N (Sept. 2019).

[6] Valsecchi, G., Bianucci, G., Marioni, F., Vernani, D., Zocchi, F. E., Korhonen, T., Pasanen, M., Pareschi, G., Ferreira, I., Bavdaz, M., and Wille, E., "Integration facility for the ATHENA X-Ray Telescope," in [*Optics for EUV, X-Ray, and Gamma-Ray Astronomy IX*], *Society of Photo-Optical Instrumentation Engineers (SPIE) Conference Series* **11119**, 111190M (Sept. 2019).

[7] Guainazzi, M., Bavdaz, M., Burwitz, V., and et al., "ATHENA Mirror Calibration Plan." ESA-ATHENA-ESTEC-SCI-PL-0001.

[8] Burwitz, V., Bradshaw, M., Eder, J., Breunig, E., Ayre, M., Bavdaz, M., and Ferreira, I., "Design of a new long beam x-ray test facility for ATHENA," in [*Society of Photo-Optical Instrumentation Engineers (SPIE) Conference Series*], *Society of Photo-Optical Instrumentation Engineers (SPIE) Conference Series* **11444**, 114444L (Dec. 2020).

[9] Pareschi, G., Moretti, A., Salmaso, B., Sironi, G., Tagliaferri, G., Uslenghi, M., Fiorini, M., Attinà, P., Bressan, R., Marchiori, G., Tordi, M., Marioni, F., Valsecchi, G., and Zocchi, F., "A vertical facility based on raster scan configuration for the x-ray scientific calibrations of the ATHENA optics," in [*International Conference on Space Optics — ICSO 2018*], *Society of Photo-Optical Instrumentation Engineers (SPIE) Conference Series* **11180**, 1118025 (July 2019).

[10] Moretti, A., Pareschi, G., Uslenghi, M., Tordi, M., Bressan, R., Valsecchi, G., Zocchi, F., Attina, P., Amisano, F., Sironi, G., Salmaso, B., Basso, S., Tagliaferri, G., Spiga, D., La Palombara, N., Fiorini, M., Dury, F., Marioni, F., Parissenti, G., Parodi, G., Wille, E., Corradi, P., Bavdaz, M., and Ferreira, I., "VERT-X: VERTical X-ray raster-scan facility for ATHENA calibration. The concept design.," in [*Optics for EUV, X-Ray, and Gamma-Ray Astronomy IX*], *Society of Photo-Optical Instrumentation Engineers (SPIE) Conference Series* **11119**, 111190O (Sept. 2019).

[11] Moretti, A., Pareschi, G., Basso, S., Spiga, D., Ghigo, M., Tagliaferri, G., Sironi, G., Civitani, M., Cotroneo, V., La Palombara, N., Uslenghi, M., Tordi, M., Delorenzi, S., Valsecchi, G., Zocchi, F., Marioni, F., Vernani, D., Amisano, F., Parissenti, G., Parodi, G., Ottolini, M., Corradi, P., Bavdaz, M., and Ferreira, I., "The VERT-X calibration facility: development of the most critical parts," in [*Society of Photo-Optical Instrumentation Engineers (SPIE) Conference Series*], *Society of Photo-Optical Instrumentation Engineers (SPIE) Conference Series* **11822**, 118220K (Aug. 2021).

[12] Biasi, R., Pescoller, D., and Rampini, F., "MicroCLINE: an innovative tiltmeter concept and its application the ALMA-EU antennas' dynamic metrology," in [*Ground-based and Airborne Telescopes III*], Stepp, L. M., Gilmozzi, R., and Hall, H. J., eds., *Society of Photo-Optical Instrumentation Engineers (SPIE) Conference Series* **7733**, 77333N (July 2010).

[13] Willingale, R., "Stray x-ray flux in the Athena Mirror," in [*Optics for EUV, X-Ray, and Gamma-Ray Astronomy IX*], *Society of Photo-Optical Instrumentation Engineers (SPIE) Conference Series* **11119**, 111190Q (Sept. 2019).

[14] Spiga, D., Moretti, A., Pareschi, G., Sironi, G., Bavdaz, M., Ferreira, I., Valsecchi, G., Marioni, F., and Zocchi, F., "Optical simulations for the Wolter-I collimator in the VERT-X calibration facility," in [*Society*

of Photo-Optical Instrumentation Engineers (SPIE) Conference Series], *Society of Photo-Optical Instrumentation Engineers (SPIE) Conference Series* **11822**, 118220L (Sept. 2021).

[15] Willingale, R., Pareschi, G., Christensen, F., and den Herder, J.-W., "The Hot and Energetic Universe: The Optical Design of the Athena+ Mirror," *arXiv e-prints* , arXiv:1307.1709 (July 2013).